Communication

A New Family of Multiferrocene Complexes with Enhanced Control of Structure and Stoichiometry via Coordination-Driven Self-Assembly and Their Electrochemistry

Hai-Bo Yang, Koushik Ghosh, Yue Zhao, Brian H. Northrop, Matthew M. Lyndon, David C. Muddiman, Henry S. White, and Peter J. Stang

J. Am. Chem. Soc., **2008**, 130 (3), 839-841 • DOI: 10.1021/ja710349j

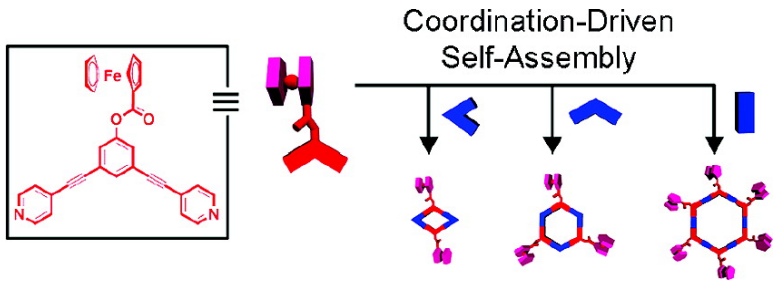

J|A|C|S
COMMUNICATIONS

Published on Web 01/01/2008

A New Family of Multiferrocene Complexes with Enhanced Control of Structure and Stoichiometry via Coordination-Driven Self-Assembly and Their Electrochemistry

Hai-Bo Yang,[†] Koushik Ghosh,[†] Yue Zhao,[†] Brian H. Northrop,[†] Matthew M. Lyndon,[§] David C. Muddiman,[§] Henry S. White,*[,†] and Peter J. Stang*[,†]

Department of Chemistry, University of Utah, 315 South 1400 East, Room 2020, Salt Lake City, Utah 84112, and W. M. Keck FT-ICR Mass Spectrometry Laboratory and Department of Chemistry, North Carolina State University, Raleigh, North Carolina 27695

Received November 15, 2007; E-mail: stang@chem.utah.edu

Molecules that exhibit multifunctionality, such as those with multiple electroactive or photoactive moieties, are of interest because of a variety of materials and synthetic applications. Ferrocene, for example, has been widely utilized in multifunctional compounds because it is a stable and readily oxidizable organometallic complex with the potential to be used in electroluminescent, information storage, and photochemical devices.[1] To date, most multifunctional ferrocenyl compounds have been prepared as, or incorporated into, polymers or dendrimers.[2] Typically synthesized using traditional covalent strategies, multifunctional polymers and dendrimers often require considerable synthetic effort and can be plagued by low yields and largely amorphous final structures. Molecular self-assembly processes offer considerable synthetic advantages including significantly fewer steps, fast and facile formation of final products, and specific, well-defined arrangements of individual components.

In the past two decades, coordination-driven self-assembly has evolved to be a well-established process for the preparation of nanoscopic supramolecular ensembles with predetermined shapes, sizes, and geometries.[3] Stimulated by the power and versatility of this paradigm, we envisioned that functionalization of a bispyridyl donor unit (Figure 1) would, when combined with appropriately designed Pt(II) acceptors, lead to the formation of a new family of multiferrocenyl rhomboidal and hexagonal structures. Moreover, this strategy allows for precise control over the shape and size of the resulting metallacycles as well as the distribution and total number of incorporated ferrocene moieties. This ability to fine-tune the size, shape, distribution, and distance between electroactive ferrocenes would help provide a greater understanding of the influence to electrochemistry caused by structural factors. This research also provides a new approach to the study of functional amplification,[4] which is a property characteristic of living systems, but so far limited to dendrimers in synthetic systems.

We have recently shown that the addition of functional groups, such as crown ethers and Fréchet-type dendrons,[5] at the vertex of 120° building units enables the preparation of novel, functionalized cavity-cored assemblies. Similarly, by attaching a ferrocene group on the periphery of a 120° donor building block it will, when combined with suitable 60°, 120°, or 180° acceptor units, give rise to rhomboidal or different sized hexagonal heterobimetallic systems. The ferrocenyl 120° donor precursor **1** can be easily prepared via a coupling reaction of ferrocene-1-carboxylic acid and 3,5-bis-(pyridin-4-ylethynl)phenol. Stirring the mixture of **1** and 60°, 120°,

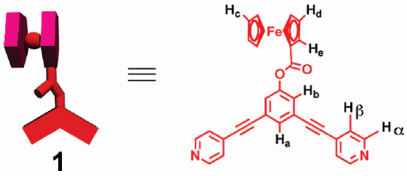

Figure 1. Schematic and molecular structure of ferrocenyl donor **1**.

Scheme 1. Molecular Structures of **2**−**4** as Well as a Graphical Representation of the Self-Assembly of Heterobimetallic Compounds **5**−**7**

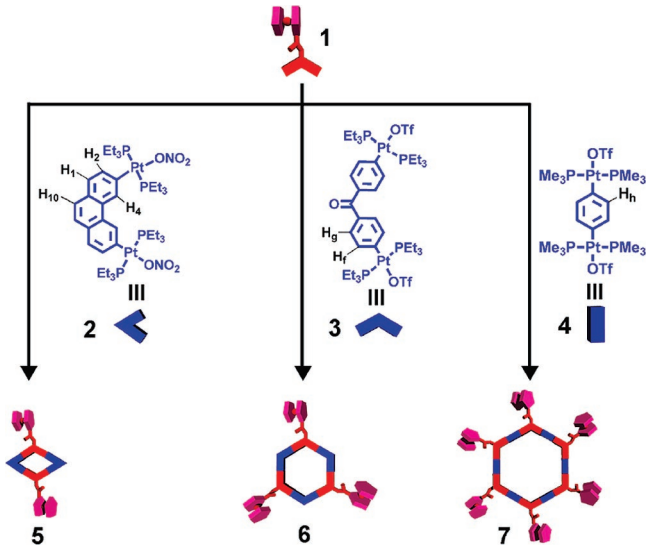

or 180° di-Pt(II) acceptor **2**, **3**, or **4** in a 1:1 ratio, respectively, resulted in the formation of the [2+2] rhomboid **5**, the [3+3] hexagon **6**, and the [6+6] hexagon **7** with pendant ferrocene groups at donor vertexes (Scheme 1).

Multinuclear NMR (^{1}H and ^{31}P) analysis (Figure 3) of the reaction mixtures revealed the formation of discrete, highly symmetric species. The ^{31}P {^{1}H} NMR spectra of **5**−**7** displayed sharp singlets (ca. 12.2 ppm for **5**, 13.5 ppm for **6**, and −14.6 ppm for **7**) shifted upfield from the peaks from the starting platinum acceptors **2**, **3**, and **4** by approximately 11.8, 6.0, and 8.3 ppm, respectively. This change as well as the decrease in coupling of flanking ^{195}Pt satellites (ca. $\Delta J = -197$ Hz for **5**, $\Delta J = -148$ Hz for **6**, $\Delta J = -79$ Hz for **7**) is consistent with back-donation from

[†] University of Utah.
[§] North Carolina State University.

10.1021/ja710349j CCC: $40.75

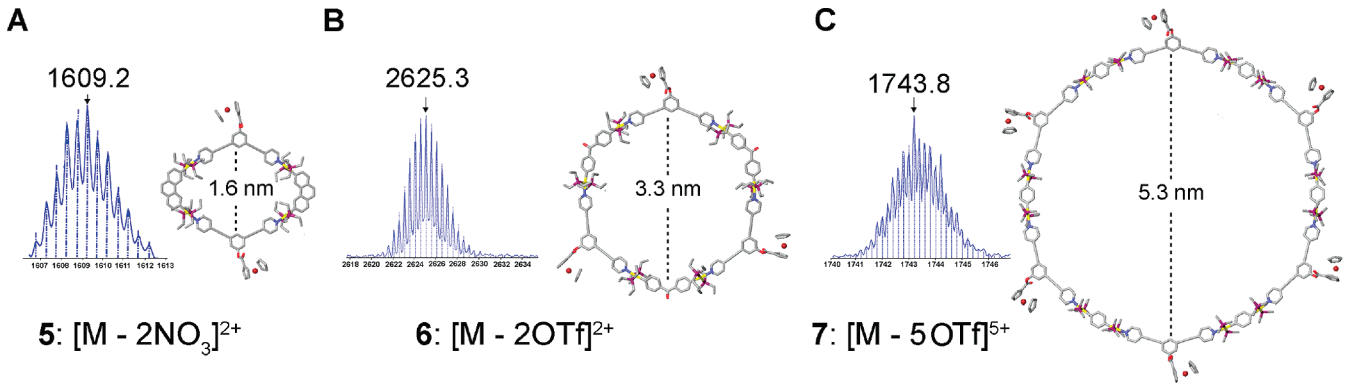

Figure 2. ESI-MS spectrum and molecular force field model of bisferrocenyl rhomboid **5** (A). ESI-TOF-MS spectra and molecular force field models of trisferrocenyl hexagon **6** (B) and hexakisferrocenyl hexagon **7** (C). For each spectrum vertical lines indicate the theoretical abundances, while the solid line is the experimental result.

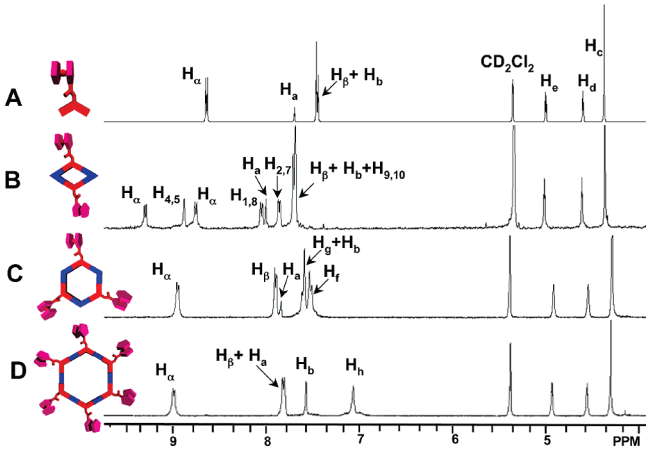

Figure 3. Partial ^{1}H NMR spectra recorded at 500 MHz (CD_2Cl_2, 298 K) of donor **1** (A), rhomboid **5** (B), and hexagons **6** (C) and **7** (D).

the platinum atoms. Additionally, the protons of the pyridine rings exhibited downfield shifts (ca. α-H_{Py}, 0.22−0.54 ppm; β-H_{Py}, 0.2−0.3 ppm), resulting from the loss of electron density upon coordination of the pyridine-N atom with the Pt(II) metal center.

ESI mass spectrometry provides further evidence for the formation of new multiferrocene systems. The ESI mass spectrum for bisferrocenyl rhomboid **4** (Figure 2A) revealed a peak at m/z = 1609.2, corresponding to $[M - 2NO_3]^{2+}$. In the ESI-TOF mass spectra of **6** and **7** (Figure 2B,C), peaks at m/z = 2625.26 and m/z = 1743.81, attributable to $[M- 2OTf]^{2+}$ for **6** and $[M - 5OTf]^{5+}$ for **7**, respectively, were observed as well. All peaks were isotopically resolved, and they agree very well with the theoretical distribution. The collective analytical results indicate that the multiferrocenyl complexes can be easily prepared (>95%) through coordination self-assembly, thus avoiding the time-consuming procedures and low yields often encountered in covalent synthesis protocols.

Table 1. Results of Electrochemical (CH_2Cl_2 with 0.1 M n-Bu_4NPF_6, 298 K) Studies of Free Ferrocene, Donor **1**, and Multiferrocenyl Compounds **5**−**7**

compound	$E_{1/2}$ (V vs Ag/AgCl)	10^6D ($cm^2 \cdot s^{-1}$)	θ_{sites}
ferrocene	0.479 ± 0.004	18 ± 1.20	1.2 ± 0.08
1	0.802 ± 0.004	8.8 ± 0.20	1.1 ± 0.03
5	0.765 ± 0.002	2.2 ± 0.21	2.0 ± 0.19
6	0.652 ± 0.003	1.4 ± 0.15	2.9 ± 0.31
7	0.644 ± 0.007	0.82 ± 0.033	5.8 ± 0.24

Molecular force-field simulations were used to gain further insight into the structural characteristics of multiferrocene complexes **5**−**7** (Figure 2). A 1.0 ns molecular dynamics simulation (OPLS force field) was used to equilibrate supramolecules **5**−**7**, followed by energy minimization of the resulting structures to full convergence. The model structure of bisferrocenyl rhomboid **4** features a well-defined rhombus with an approximately 2.4 × 1.6 nm cavity. Likewise, simulations revealed very similar planar hexagonal structures for trisferrocenyl hexagon **6** and hexaferrocenyl hexagon **7**, yet different sized cavities (3.3 × 3.1 nm for **6**, 5.3 × 5.1 nm for **7**).

Cyclic voltammetry of ferrocenyl donor **1** as well as multiferrocene complexes **5**−**7** was performed in a dichloromethane solution containing 0.1 M n-Bu_4NPF_6 as the supporting electrolyte using a ~1 mm^2 Pt disk electrode.[6] The cyclic voltammograms corresponding to the one-electron oxidation of the ferrocene groups yielded anodic/cathodic peak current ratios of $i_a/i_c \approx 1$ (Figure 4A,B). The half-wave potential, $E_{1/2}$, measured as the average of the anodic and cathodic peak potentials, are presented in Table 1. The difference between the anodic and cathodic peak potentials (ΔE_p) was found to be larger than the theoretical value of 59 mV

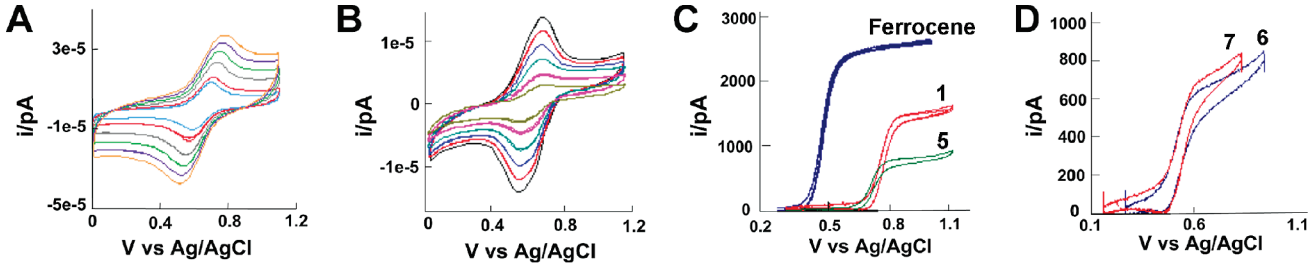

Figure 4. Cyclic voltammograms of 0.20 mM **6** (A) and 0.21 mM **7** (B) at a scan rate of 25−250 mV/s. Steady-state response on a Pt ultramicroelectrode at a scan rate of 20 mV/s for 0.22 mM Fc, 0.20 mM **1**, **5**, and **6**, and 0.21 mM **7** (C, D) in CH_2Cl_2 containing 0.1 M n-Bu_4NPF_6.

expected for a reversible one-electron redox reaction,[7] a consequence of the solution ohmic resistance.[8]

To gain additional insight into the structure and electronic properties of **5**−**7**, potential-step chronoamperometry at a 25-μm-diameter Pt disk electrode was performed to determine the diffusion coefficient, *D*, for each compound. The method of Denault et al.[9a] was employed, which does not require *a priori* knowledge of the number of ferrocene sites per molecule, θ_{sites}, or the redox concentration.[9] The current $i(t)$ was monitored as a function of time following a rapid change of the electrode from a value where no reaction occurs to a value where the ferrocenyl groups are oxidized at the diffusion-controlled rate. The slope of the linear region of plots of $i(t)/i_{lim}$ versus $t^{-1/2}$, where i_{lim} is the steady-state current at long times, directly yielded values of *D* for each compound. (see Supporting Information for details). The results are reported in Table 1. The ratio of the diffusion coefficients of rhomboid **5**, triferrocenyl hexagon **6**, and hexaferrocenyl hexagon **7** is 3.0:1.8:1.0, indicating that their hydrodynamic diameters lie in the inverse ratio of 1:1.7:3.0, since *D* is inversely proportional to the molecular size. Molecular force field simulations showed outer diameters of about 3.0, 4.2, and 6.9 nm for **5**, **6**, and **7**, respectively, which are in relative, qualitative agreement with the experimentally determined ratio (Figure 2).

With knowledge of the values of *D* obtained from the above chronoamperometric experiments, the number of the electroactive sites for compounds **5**−**7**, which are assumed to have 2, 3, and 6 ferrocenyl groups, could be independently determined. The steady-state limiting current obtained from Pt microdisk electrodes (Figure 4C,D), could be used to calculate θ_{sites} using the expression $i_{lim} = 4nFDaC\theta_{sites}$, where *n* is the number of electrons transferred per ferrocenyl site (=1), *F* is the Faraday constant, *C* is the bulk concentration, θ_{sites} is the number of reactive ferrocenyl sites per molecule, and *a* is the radius of the electrode.[10] Experimentally measured values of θ_{sites} (Table 1) for compounds **5**−**7** agree with the expected values of 2, 3, and 6, demonstrating that all ferrocenyl groups attached to the metallacycles are electroactive.

Considering the expected absence of strong intramolecular electronic coupling bridges between the ferrocenes in the structures of assemblies **5**−**7**, independent, one-electron oxidations are expected to be observed when analyzing the waveshape of steady-state voltammograms plotted as $\log[(i_{lim} - i)/i]$ versus E.[11] The calculated slopes of **5**, **6**, and **7** are 52, 56, and 54 mV, which are near the ideal value (0.059/*n* with $n = 1$), indicating that the redox species react one-at-a-time, more or less independently of one another.

In conclusion, we present a facile and versatile strategy for the synthesis of multiferrocenyl complexes where coordination-driven self-assembly allows precise control over metallacycle shape and size and the distribution of ferrocene moieties. Electrochemical studies reveal that all of the redox sites attached to complexes **5**−**7** are stable, independent, and electrochemically active and display 2, 3, and 6 reaction sites, respectively. All heterobimetallic compounds show one-electron reaction responses, with the additional electroactive sites enhancing the magnitude of current. Furthermore, the increased size of the assemblies also results in a decrease in the diffusion coefficient, *D*. These findings provide an enhanced understanding of the influence of structural factors on the electrochemistry of multifunctional electroactive supramolecular metallacycles, which can be easily prepared by coordination-driven self-assembly, and make them of interest as potential multielectron redox catalysts, electron reservoirs, electrode modifiers, ion sensors, mimics of biological redox processes, etc.

Acknowledgment. P.J.S. thanks the NIH (Grant GM-057052) and the NSF (Grant CHE-0306720) for financial support. B.H.N. thanks the NIH (Grant GM-080820) for financial support. H.S.W. thanks the NSF (Grant CHE-0616505) for financial support. D.C.M. and M.M.L. thank NCBC and NCSU for generous financial support.

Supporting Information Available: Synthesis and analytical data of **1** and **5**−**7**; cyclic voltammetric, steady-state measurements, chronoamperometry, calculations of *D* and θ_{site}, and molecular modeling procedures. This material is available free of charge via the Internet at http://pubs.acs.org.

References

(1) (a) Sun, S.-S.; Lees, A. J. *Inorg. Chem*. **2001**, *40*, 3154. (b) van Staveren, D. R.; Metzler-Nolte, N. *Chem. Rev.* **2004**, *104*, 5931. (c) You, C.-C.; Wurthner, F. *J. Am. Chem. Soc*. **2003**, *125*, 9716. (d) Shoji, O.; Okada, S.; Satake, A.; Kobuke, Y. *J. Am. Chem. Soc*. **2005**, *127*, 2201. (e) Das, N.; Arif, A. M.; Stang, P. J.; Sieger, M.; Sarkar, B.; Kaim, W.; Fiedler, J. *Inorg. Chem*. **2005**, *44*, 5798. (f) Chebny, V. J.; Dhar, D.; Lindeman, S. V.; Rathore, R. *Org. Lett*. **2006**, *8*. 5041. (g) Mereacre, V.; Nakano, M.; Gomez-Segura, J.; Imaz, I.; Sporer, C.; Wurst, K.; Veciana, J.; Turta, C.; Ruiz-Molina, D.; Jaitner, P. *Inorg. Chem*. **2006**, *45*, 10443. (h) Collinson M. M. *Acc. Chem. Res*. **2007**, *40*. 777. (i) Lang, H.; Packheiser, R. *Collect. Czech. Chem. Commun*. **2007**, *72*, 435.

(2) (a) Fréchet, J. M. *Science* **1994**, *263*, 1710. (b) Rulkens, R.; Lough, A. J.; Manners, I.; Lovelace, S. R.; Grant, C.; Geiger, W. E. *J. Am. Chem. Soc*. **1996**, *118*, 12683. (c) Valerio, C.; Fillaut, J.-L.; Ruiz, J.; Guittard, J.; Blais, J.-C.; Astruc, D. *J. Am. Chem. Soc*. **1997**, *119*, 2588. (d) Castro, R.; Cuadrado, I.; Alonso, B.; Casado, C. M.; Moran, M.; Kaifer, A. E. *J. Am. Chem. Soc*. **1997**, *119*, 5760. (e) Anicet, N.; Anne, A.; Moiroux, J.; Savéant, J.-M. *J. Am. Chem. Soc*. **1998**, *120*, 7115. (e) Nlate, S.; Ruiz, J.; Blais, J.-C.; Astruc, D. **2000**, 417. (f) Nguyen, P.; Gomez-Elipe, P.; Manners, I. *Chem. Rev*. **1999**, *99*, 1515. (g) Brinke, G.; Ikkala, O. *Science* **2002**, *295*, 2407. (h) Stone, D. L.; Smith, D. K.; McGrail, P. T. *J. Am. Chem. Soc*. **2002**, *124*, 856. (i) Choi, T.-L.; Lee, K.-H.; Joo, W.-J.; Lee, S.; Lee, T.-W.; Chae, M. Y. *J. Am. Chem. Soc.* **2007**, *129*, 9842.

(3) (a) Stang, P. J.; Olenyuk, B. *Acc. Chem. Res.* **1997**, *30*, 502. (b) Leininger, S.; Olenyuk, B.; Stang, P. J. *Chem. Rev.* **2000**, *100*, 853. (c) Seidel, S. R.; Stang, P. J. *Acc. Chem. Res.* **2002**, *35*, 972. (d) Schwab, P. F. H.; Levin, M. D.; Michl, J. *Chem. Rev.* **1999**, *99*, 1863. (e) Holliday, B. J.; Mirkin, C. A. *Angew. Chem., Int. Ed.* **2001**, *40*, 2022. (f) Cotton, F. A.; Lin, C.; Murillo, C. A. *Acc. Chem. Res.* **2001**, *34*, 759. (g) Fujita, M.; Tominaga, M.; Hori, A.; Therrien, B. *Acc. Chem. Res.* **2005**, *38*, 369. (h) Fiedler, D.; Leung, D. H.; Bergman, R. G.; Raymond, K. N. *Acc. Chem. Res.* **2005**, *38*, 349.

(4) (a) de Groot, F. M. H.; Albrecht, C.; Koekkoek, R.; Beusker, P. H.; Scheeren, H. W. *Angew. Chem., Int. Ed.*. **2003**, *42*, 4490. (b) Amir, R. J.; Pessah, N.; Shamis, M.; Shabat, D. *Angew. Chem., Int. Ed.* **2003**, *42*, 4494. (c) Li, S.; Szalai, M. L.; Kevwitch, R. M.; McGrath, D. V. *J. Am. Chem. Soc*. **2003**, *125*, 10516.

(5) (a) Yang, H.-B.; Das, N.; Huang, F.; Hawkridge, A. M.; Muddiman, D. C.; Stang, P. J. *J. Am. Chem. Soc.* **2006**, *128*, 10014. (b) Yang, H.-B.; Hawkridge, A. M.; Huang, S. D.; Das, N.; Bunge, S. D.; Muddiman, D. C.; Stang, P. J. *J. Am. Chem. Soc*. **2007**, *129*, 2120. (c) Yang, H.-B.; Ghosh, K.; Northrop, B. H.; Zheng, Y.-R.; Lyndon, M. M.; Muddiman, D. C.; Stang, P. J. *J. Am. Chem. Soc*. **2007**, *129*, 14187.

(6) The complexes remain unchanged before and after the cyclic voltametry measurement as indicated by NMR analysis.

(7) Matsuda, H.; Ayabe, Y.; *Z. Electrochem*. **1955**, *59*, 494.

(8) It is not uncommon for the resistance to be in the range of several kΩ even with 0.1 M supporting electrolyte.

(9) (a) Denault, G.; Mirkin, M.; Bard, A. J. *J. Electroanal. Chem.* **1991**, *308*, 27. (b) Biondi, C.; Bellugi, L. *J. Electroanal. Chem*. **1970**, *24*, 263. (c) Amatore, C.; Azzali, M.; Calas, P.; Jutand, A.; Lefrou, C.; Rollin, Y. J. *Electroanal. Chem.* **1990**, *288*, 45. (d) Mirkin, M. V.; Nilov, A. P. *J. Electroanal. Chem.* **1990**, *283*, 35. (e) Nowinski, S. A.; Anjo, D. M. *J. Chem. Eng. Data* **1989**, *34*, 265.

(10) Bard, A. J.; Faulkener, L. R. *Electrochemical Methods: Fundamentals and Applications;* Wiley: New York, 1980.

(11) (a) Miles, D. T.; Murray, R. W. *Anal. Chem.* **2001**, *73*, 921. (b) Templeton, A. C.; Cliffel, D. E.; Murray, R. W. *J. Am. Chem. Soc.* **1999**, *121*, 7081.

JA710349J